PID Control of a Novel Variable Reluctance Gripper

Norbert C. Cheung, *Member, IEEE* and Kenneth Kin-Chung Chan, *Student, IEEE*

***Abstract*-- Material handling and pick and place mechanisms are widely found in factory automation and industrial manufacturing. Mechanical grippers based on different motor technologies have been designed and employed numerous applications. However, variable reluctance (VR) technology is never explored. This is due to its inherent nonlinear control characteristics.**

The paper describes the motion control of a novel two-finger gripper using VR technology. A novel two-finger VR gripper is proposed and fabricated. A mathematical model of the actuator is constructed. A novel motion control strategy is proposed. Finally, the simulation and implementation of the VR gripper are carried out. Results show that the proposed actuator is an ideal solution for low-cost and high precision gripping applications.

***Index terms*-- Variable Reluctance Motor, gripper control.**

I. Introduction

Gripping mechanism plays an important role in material handling, automation and product manufacturing. In many industries, like the semiconductor packaging industry, the applications become increasingly demanding as their product technologies advance. These lay pressure to their manufacturing machineries. A low-cost and robust motion-system solution with high performance and reliability must be developed for these machineries.

Recently years, various gripper designs were tailor-made for numerous requirements. Actuators ranging from simple and fast response DC permanent motors to slow response thermal actuators were used [1-2]. However, actuators based on variable reluctance (VR) technology were never explored.

VR actuator is inherently simple and robust in structure, due to the absence of permanent magnet. It has high-energy conversion efficiency and it is capable to operate in hostile and extreme temperature situations. Nevertheless, the non-linearity caused by its magnetic characteristics has been a major drawback, and has kept it from wide acceptance in industry. With the dramatic increase in the processing power of Digital Signal Processors (DSP) and reduction in price of these components, advanced control algorithm can be employed, and thus VR motors begin to regain interest.

This paper presents a novel two-finger VR gripper. The structure this device is described in section II. The modelling and the magnetic characterisation of the VR gripper are developed in sections III and IV respectively. A suitable control strategy for the VR gripper is proposed in section V. The proposed control strategy is simulated and studied in section VI. The actual hardware implementation is described in section VII. The results shown in section VIII confirmed that the VR gripper is suitable for high performance gripping motions.

II. Construction Of VR Gripper

Fig. 1 shows the construction of the two-finger VR gripper. It consists of two rotary elements, each attached to a finger. The actuator contains two coils, each with a 400-turn winding.

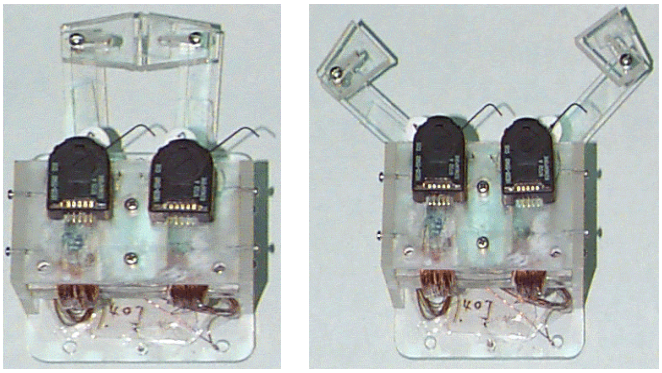

(a) at aligned (grasp) position (b) at unaligned (release) position

Fig. 1. The VR Finger Gripper

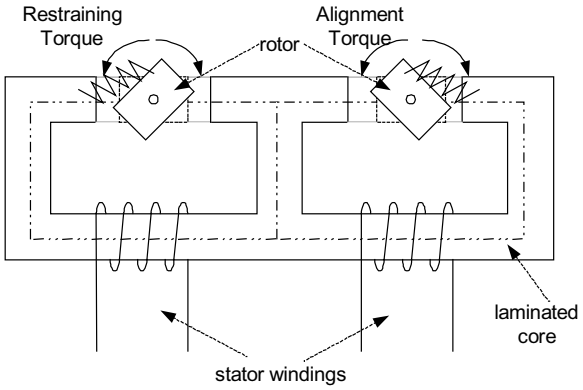

Fig. 2. Top View of Rotary VR Gripper

Norbert C. Cheung and Kenneth Kin-Chung Chan are with the Department of Electrical Engineering, Hong Kong Polytechnic University, Hong Kong SAR, China. (e-mail: eencheun@inet.polyu.edu.hk)

The moving rotors are mounted onto two individual shafts, whose axes are normal to the plane of the diagram, so that the moving elements may rotate freely between the poles of the stator. Both the rotors and stators are made up of laminated mild steel to reduce eddy currents.

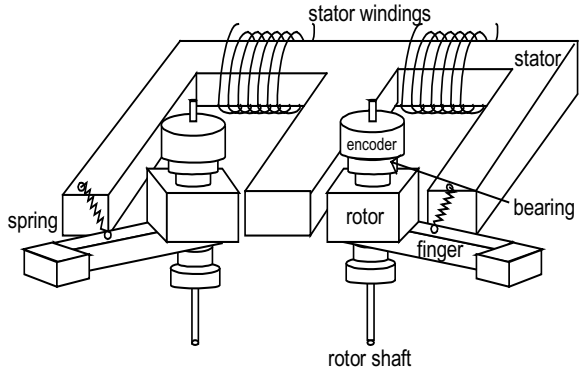

Fig. 3. Side View of Rotary VR Gripper.

The two fingers of the gripper, shown in Fig. 3, are 90mm long and are spring loaded. This arrangement allows bi-directional movement from a single-direction coil excitation. When currents are applied to the stator windings, the rotors will rotate away from initial rest positions to reduce their reluctance by alignment torque. The rotors will stop when alignment torque comes into equilibrium with restraining torque provided by the spring. When the fingers rotate by 70°, the fingertips would be closed and the rotors are in fully aligned positions. Incremental rotary encoders are mounted on the actuator's shafts to measure the rotor positions with a resolution of 0.09°.

III. MODELLING

The motor characteristics can be described by equations below:

$$J_j \frac{d^2\theta_j}{dt^2} = T_j - K_{sj}\theta_j \Big|_{j=1,2} \quad (1)$$

$$T_j = \frac{d\lambda_{jj}}{d\theta_j} i_j + \frac{d\lambda_{jk}}{d\theta_j} i_k \Big|_{j=1,2;k=2,1} \quad (2)$$

where J_j, T_j, K_{sj}, θ_j, λ_{jj}, λ_{jk} and i_j are rotor inertia, motor torque, spring constant, rotor angle, self flux linkage, mutual flux linkage and stator current respectively [3-4].

On the electrical side, the motor can be represented as a resistive and inductive structure. Its voltage equation can be expressed as:

$$V = Ri + \frac{d\lambda}{dt} \quad (3)$$

where *V, R and* λ are terminal voltage, coil resistance and flux linkage respectively. Therefore, the voltage equation can be rewritten as:

$$V_j = R_j i_j + \frac{d\lambda_{je}}{dt} + \frac{d\lambda_{jj}}{dt} + \frac{d\lambda_{jk}}{dt} \Big|_{j=1,2;k=2,1} \quad (4)$$

where λ_{je} is the leakage flux.

Note that, in the above equations [1-4], the flux linkage has a non-linear relation with current and position. With accurate flux measurement, an accurate model for the VR gripper can be obtained.

IV. MAGNETIC CHARACTERISATION

The gripper magnetic characteristic is measured by feeding AC current into the stator windings with an isolated-autotransformer from 0.5-4Amps. Flux $\Phi(t)$ is measured with search coil of N_s turns wounded around the iron core with equations below:

$$\Phi(t) = -\frac{1}{N_s} \int e(t) \cdot dt \quad (5)$$

where *e(t)* is the voltage induced by the flux

Flux linkage $\lambda(t)$ can be expressed as

$$\lambda(t) = N \cdot \Phi(t) \quad (6)$$

where *N* is the number of turns of the stator winding.

Fig. 4 shows the flux linkage hystersis loops of the VR gripper with different rotor positions. Fig. 5 shows the flux linkage hystersis loops of the VR gripper with different current levels.

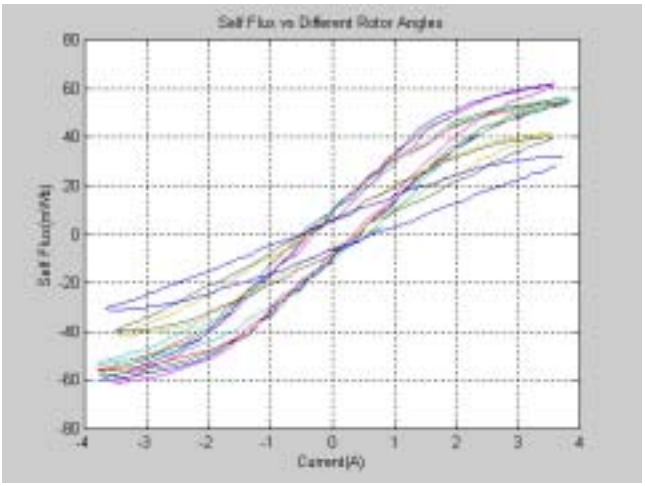

Fig. 4. Self Flux linkage versus different rotor positions

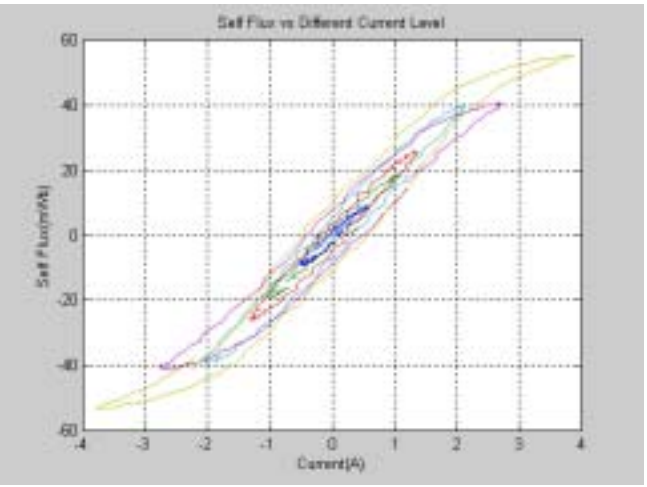

Fig. 5. Self Flux linkage versus different current level

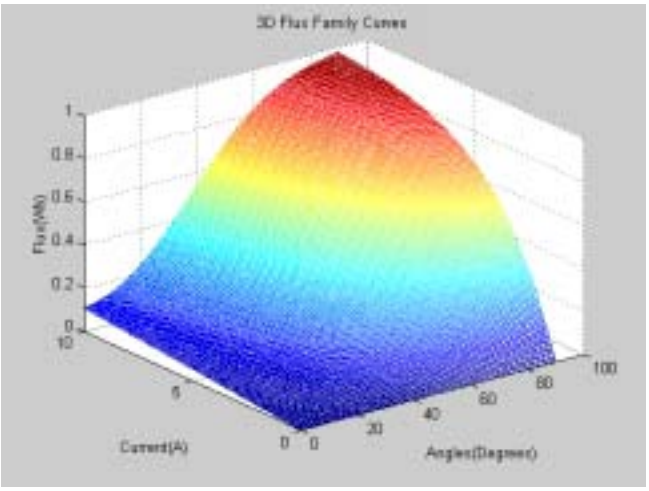

Fig. 6. 3D-Flux linkage profile of VR Gripper

An exponential flux model employed is shown as equation (6) below [5]. Then a least square non-linear two-dimensional surface fitting method is applied to the flux-current chart so that the non-linear function λ can be represented by the following equation:

$$\lambda(\theta,i) = \lambda_s(1-e^{-f(\theta)i}) \qquad (6)$$

where $f(\theta) = a + b\cos\theta + c\cos 2\theta + d\sin\theta + e\sin 2\theta$, θ is rotor angle and λ_s is a constant, of which the magnitude is equal or greater than the saturation flux of the motor.

Fig. 6 shows the 3D flux linkage profile, which is constructed by minimizing the sum-square error of its norm.

Fig. 7 shows the equivalent VR Gripper magnetic circuit representation. The stator coils, rotor and E-core common path can be represented by MMF sources, variable reluctance and fixed reluctance.

Due to the symmetrical structure of the actuator, the excitation currents in gripping motion in both stator windings and the MMF sources, Φ_l and Φ_r are assumed to be equal. Therefore, self inductance of both rotors with magnetic flux path ABD and CBD are equal. Mutual inductance would cancel each other out since they are in opposite directions [6].

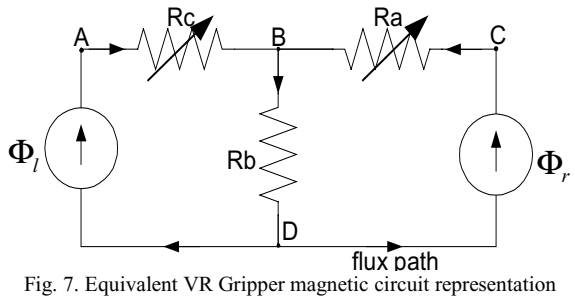

Fig. 7. Equivalent VR Gripper magnetic circuit representation

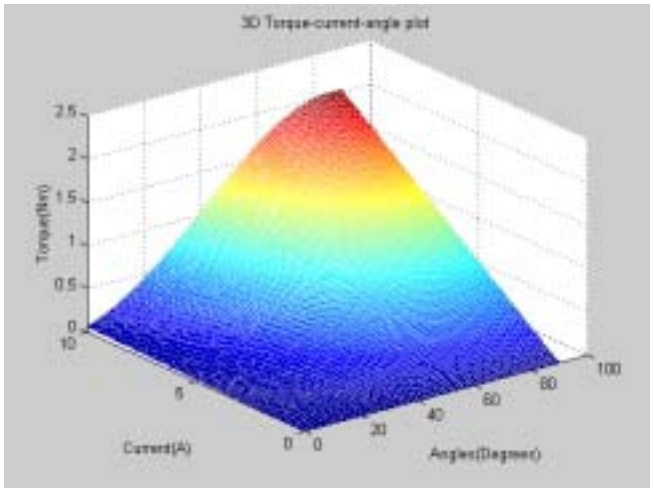

Fig. 8. 3D Torque profile of VR Gripper

Besides, with the experimental data obtained previously, 3D torque profile can be constructed with equation (2) as shown in Fig. 8. Fig. 9 shows the VR gripper torque family curves.

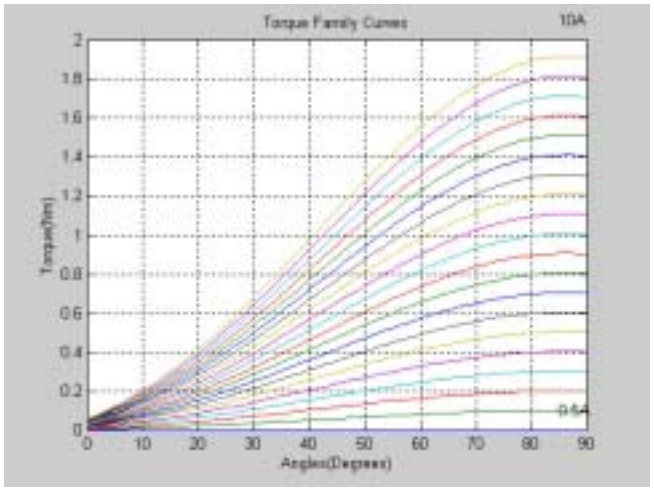

Fig. 9. VR Gripper Torque Family Curves

V. CONTROL STRATEGY

Exploiting the fact that the current dynamics is at least an order faster than the mechanical dynamics, this paper proposes a dual rate cascade control approach. A fast inner loop current controller is employed to regulate the current-voltage non-linearity of the actuator with 5kHz sampling rate, while a slower outer loop trajectory controller is used

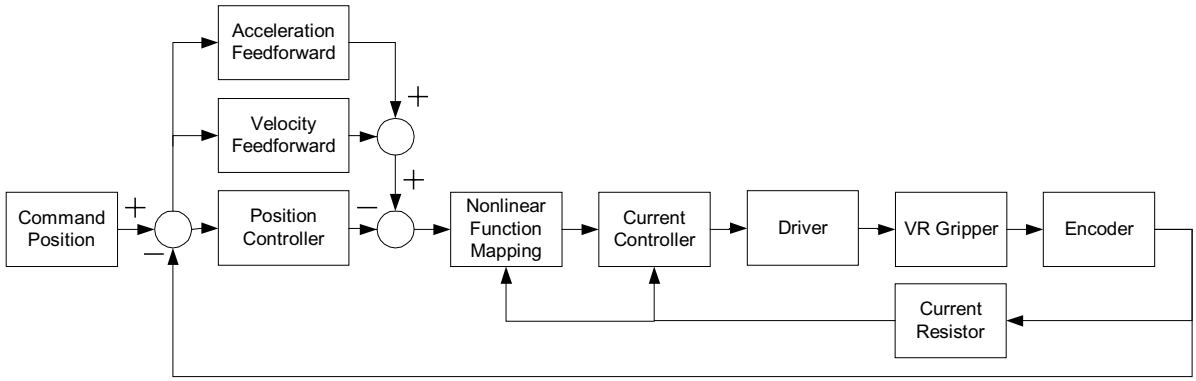

Fig. 10. Overall Control Block Diagram

to control the mechanical dynamics with 1kHz. On top of this, a non-linear function is included to compensate the non-linearity of torque against current and position.

A current controller is employed to linearise the current-voltage relation of the actuator. A PI controller is adopted to improve current response [7]. The non-linear function bridges the link between the trajectory controller and the current controller. It receives torque commands and position information, and outputs desired current set points to the current controller. Trajectory controller is employed which is a typical PID controller with feedforward component. Fig. 10 is the overall block diagram of the control system [8].

Fig. 11 shows the method of obtaining the required current i^* by bi-linear interpolation. Firstly, from the position θ_{in} and torque T_{in} inputs, two pairs of data in the look-up table $i(T_1,\theta_1)$, $i(T_2,\theta_1)$ and $i(T_1,\theta_2)$, $i(T_2,\theta_2)$ are located. For each pair, a linear interpolation is done, according to the ratio of T_1, T_2, and T_{in}. As a result two intermediate elements $i(T_{1\text{-}2},\theta_1)$ and $i(T_{1\text{-}2},\theta_1)$ are obtained. Finally, the output current command i^* is obtained by interpolating the two intermediate elements with θ_1, θ_2, and θ_{in}.

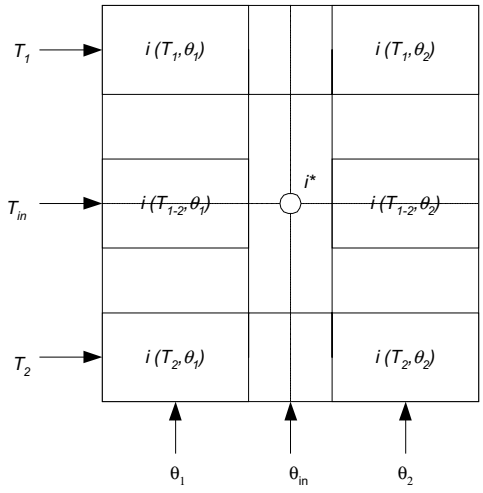

Fig. 11. Calculating i^* from the look-up table

Fig 12 shows the torque profile required to generate the lookup table mentioned above. The torque ranges from 0.1Nm to 1.6Nm with maximum current of 10A.

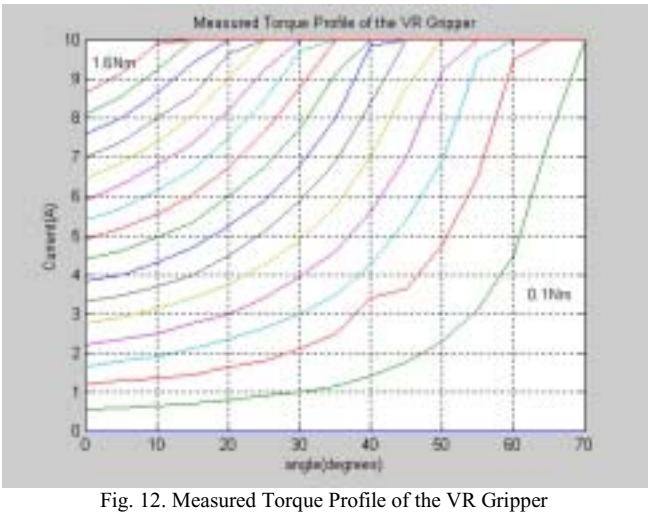

Fig. 12. Measured Torque Profile of the VR Gripper

The controller's operation is based on the assumption that the current controller has perfect tracking capability, and the non-linear torque to current look up table generates the linearised current command to the current controller.

VI. Simulation

Sinusoidal and step position commands are fed into the model and the tracking and current responses are simulated in Fig. 13 and 14 respectively. A Matlab SIMULINK software package is used for simulation and its block diagram is shown as the Fig. 15.

Simulation results show that the actuator is capable in achieving high precision. However, a sharp overshoot in position and high current consumption can be resulted with a step command input. A profile is required to provide a swift settling time and reduce the stress on mechanical systems.

Besides, a large derivative term is introduced to provide a fast dynamic response, which brings along small amplitude oscillations at settling. A smaller derivation term was chosen to avoid unnecessary vibrations.

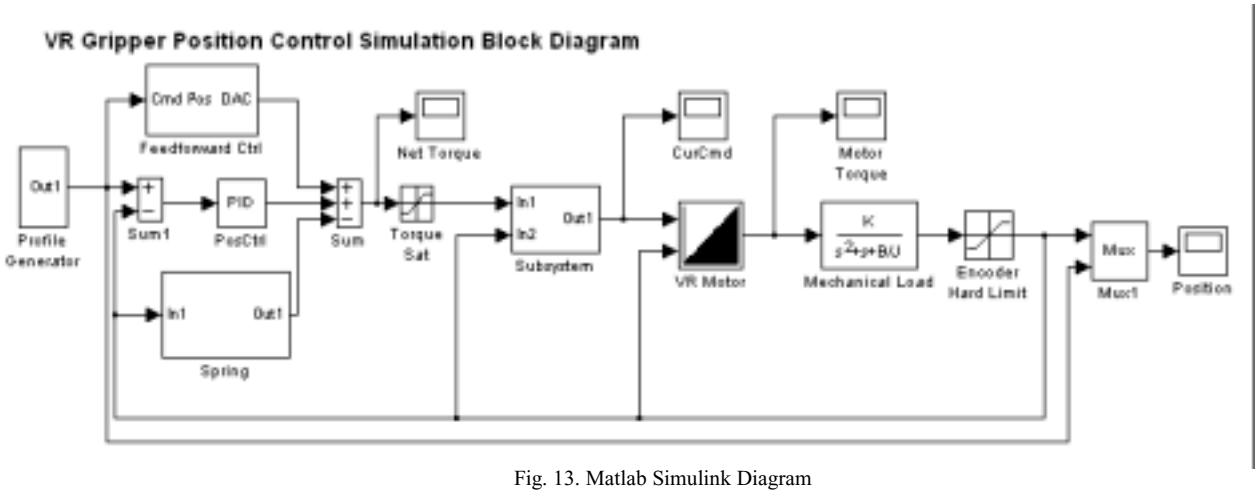

Fig. 13. Matlab Simulink Diagram

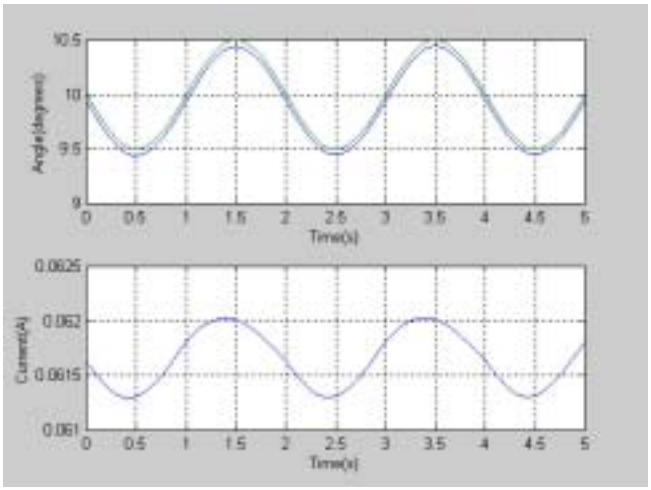

Fig. 14. Simulated Sinusoidal Response

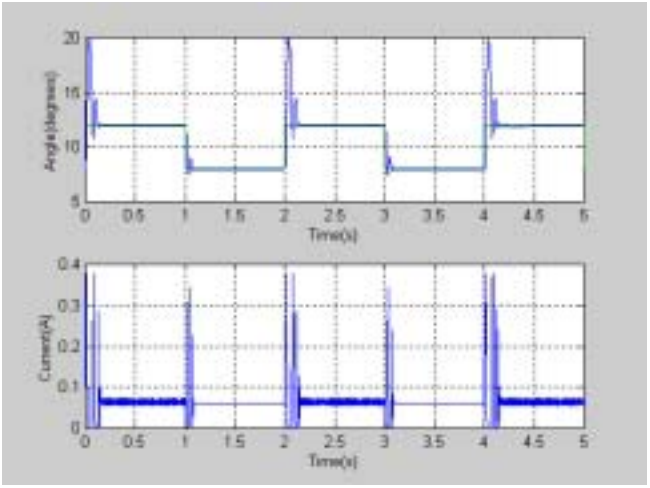

Fig. 15. Simulated Step Response

VII. Implementation

A dSPACE DS1102 card is used as the motion controller. The card has an on-board 60MHz TMS320C31 DSP for real-time computation and interfaces with the PC through the ISA bus. It consists of two 24bits incremental encoder input channels, two 12 bits ADC channels and six PWM channels. In connecting with MATLAB real-time workshop and SIMULINK, real-time control C-code can be generated with a SIMULINK diagram. Assembly codes can be compiled and downloaded to the DSP.

The digital control PWM driver used in this project is a pair of MOSFET half-bridge driver as shown in Fig. 16. It acts as a current amplifier for the VR gripper. It has fewer components than the full bridge amplifier and has a true ground that makes current measurement much simpler. Current measurement is then fed back to analogue input for current loop control.

The motor side & logic side is electrically isolated by the opto-couplers. Dead-time delay protection against cross conduction of the high-low side MOSFETS is introduced. The chopping frequency is set at 24kHz to ensure good current dynamics.

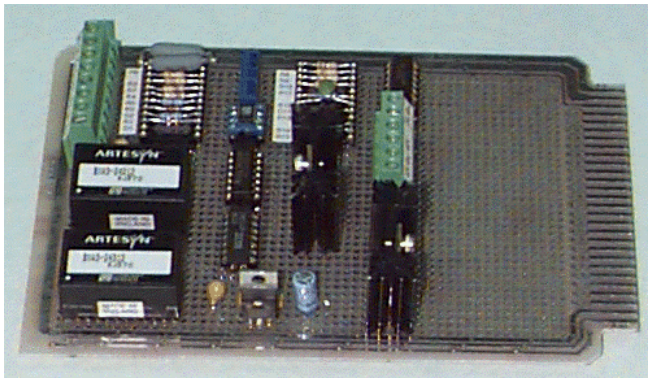

Fig. 16. Prototype PWM Half Bridge Amplifier

The rotary incremental encoder is connected with the encoder input channels for position control. Fig. 17 shows the system configuration with dSPACE controller card.

VIII. Experimental Results

A. Current Loop Responses

For the VR gripper, stator inductance varies along with rotor position. It is essential to verify its current loop stability and responses at different rotor positions. Current

responses at fully aligned and unaligned positions are investigated.

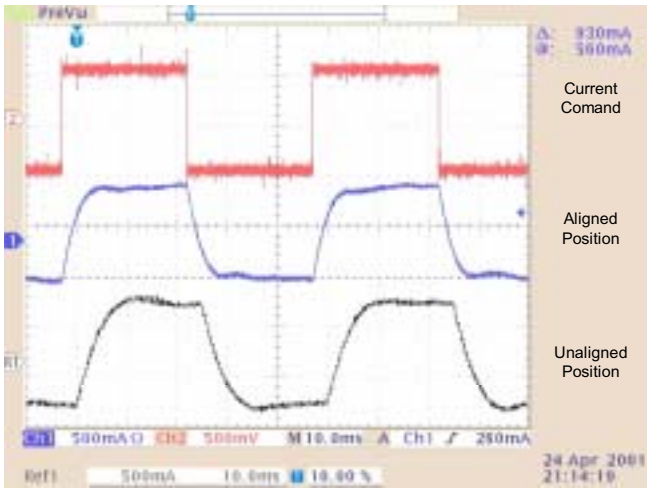

Fig. 17. 1A Current response at aligned (blue) and unaligned positions (black)

As shown in Fig. 18, there is no current instability found, while current responses at unaligned and aligned positions show fast dynamics.

B. *Position Loop Responses*

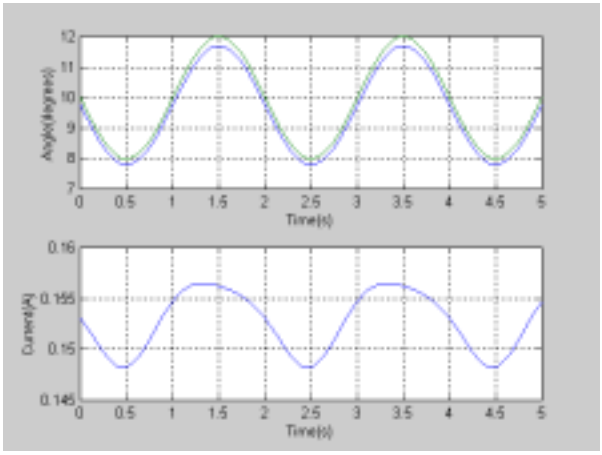

Fig. 18. Sine Wave Response

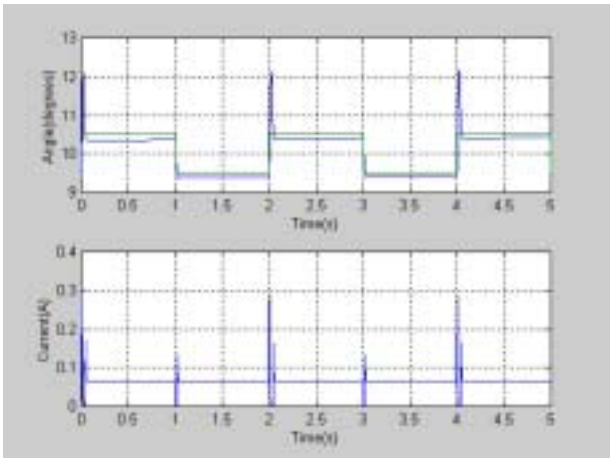

Fig. 19. Step Response

Actual response is shown in Fig. 19 and 20. The trajectory response matches closely with the simulated response while the extra current input is used to compensate the friction due to the mechanical misalignment, which is assumed to be zero in the model. Besides, the frictional effect reduces the vibration effect of the actuator.

IX. Conclusion

A novel two-finger gripper based on variable reluctance technology has been designed and fabricated. The resulting actuator is robust and simple, and it is suitable for hazardous environment. With the absence of permanent magnet, the manufacturing cost and difficulty are much reduced.

Flux linkages are measured and 3D-flux linkage profiles are generated. The actuator inherits a non-uniform force profile as a reluctance actuator.

A dynamic nonlinear model of the VR gripper is developed, which is further simulated with a proposed control algorithm. Finally, the VR gripper is controlled with PWM driver and a DSP controller. Results show that the VR Gripper is suitable for high-precision applications.

X. References

[1] H.Du, C.Su M.K. Lim, W.L. Jin, "A micromachined thermally-driven gripper: a numerical and experimental study", Smart Material Structure Vol.8, p616-622, 1999.

[2] R.D. Lorenz, J.J. Zik, D.J. Sykora, "A Direct-Drive, Robot Parts, and Tooling Gripper with High-Performance Force Feedback Control", IEEE Trans. on Indust. Appl., March/April, Vol. 27, No. 2, p275-281, 1991.

[3] T.J.E. Miller. *Switched reluctance motor and their control,* Magne Physics Publishing and Clarendon Press, Oxford, 1993.

[4] G.R. Slemon and A. Staughen. *Electric Machines.* Addison Wesley, 1982.

[5] S. Mir, I. Husain and M. E. Elbuluk. *Switched Reluctance Motor Modelling with On-Line Parameter Identification* IEEE Trans. on Ind. App., Vol. 34, No. 4, pp776-783, Jul./Aug. 1998.

[6] Fitzgerald, A.E. & Kingsley, Jr., "Electric Machinery," McGraw-Hill, 2nd Edition, 1961.

[7] K. Russa, I. Husain and M. Elbuluk. Torque Ripple Minization in Switched Reluctance Machines Over a Wide Speed Range. *IEEE Industry Applications Society Annual Meeting*, Oct., 1997. P668-675.

[8] K.W. Lim, N.C. Cheung and M.F. Rahman. *Proportional Control of a Solenoid Actuator.* IEEE Industrial Electronics Society Annual General Meeting, 1994.